https://doi.org/10.56452/2022-12-003

ISSN: 0974-5823 Vol. 7 No. 12 December, 2022

International Journal of Mechanical Engineering

IMPLEMENTATION OF SLIDING MODE CONTROL OF PWM DUAL INVERTER – BASED GRID-CONNECTED PV SYSTEM: MODELLING AND PERFORMANCE ANALYSIS

[1]Banapuram Anusha, [2] DR.C.N. Ravi

[1]M. Tech Student, [2]Professor

Department Of Electrical & Electronics Engineering

Vidya Jyothi Institute of Technology, Hyderabad

Abstract: In this article, a novel sliding-mode (SM) controller for a grid-connected photovoltaic (PV) system based on cascaded two-level inverters is presented (CTLI). A CTLI-based grid-connected PV system that converts solar radiation into active and reactive electricity via modelling and design was developed. The capability of the PV to provide its maximum power is taken into account while designing a vector controller. Two different switching mechanisms were taken into consideration and studied while building SM controllers for comparable operating scenarios. Instead of the previously stated space vector pulse width modulation (PWM) method, the suggested SM controller functions using a straightforward PWM modulation strategy. The effectiveness of the SM controller is enhanced by the use of adaptive hysteresis band computation. For both systems working with the stated load and various insolation levels in the simulated scenario, the controller's performance is assessed as excellent. It is discovered that the laboratory model can successfully perform the control algorithm in the designated context when utilised in combination with the suggested controller.

"Index Terms: Sliding-mode control (SMC), vector control, and distribution static compensator (distribution STATCOM)".

1. INTRODUCTION

Solar Photo Voltaic (SPV) systems are becoming more and more popular on a global scale as a reliable and cost-effective way to generate electricity. The fundamental benefits of SPV systems are their ability to produce clean energy from renewable resources without the need of fuel other than abundant sunshine. Depending on the availability or intensity of the solar irradiation, the SPV systems are capable of producing proportionate amounts of electrical power. When compared to other power producing systems, they don't need extensive run-time monitoring. Since the solar irradiance and ambient temperature are affected by the surrounding environment, they determine how much electrical power is produced by the SPV power conversion system. The two environmental elements have a significant impact on the SPV system's features, and they also change the system's internal properties. As a result, a maximum power point tracking (MPPT) system is necessary. The suggested effort aims to enhance the system's power quality, therefore strategies for enhancing THD, cutting losses, and PWM are prioritized. All studies are performed under the Standard test conditions (STC), which are 1000W/m2 of radiation and 25 °C of temperature. In order to guarantee the collection of the most electricity for the specified solar irradiation and temperature, Whei-Min Lin et al. (2011) adopted the MPPT technique. The Perturb and Observe (P&O), Incremental Conductance (INC), Learned Incremental Conductance (LIC), and Sliding Mode Controller (SMC) are some of the most well-known MPPT methods. K.Jyotheeswara Reddy and colleagues (2018) There are additional soft

computing-based MPPT strategies for MPPT. While most applications demand ac, the SPV-based electrical power production method generates dc output. In order to generate an ac voltage or current source with the proper amplitude, phase, and frequency, an inverter must be utilised in conjunction with the SPV system.

There are two alternative SPV system configurations: one has a battery backup while the other does not. Battery backup is used by standalone systems that demand constant power sources. Backup mechanisms are not necessary for systems designed to integrate captured electricity into the grid. Mahfuz-Ur-Rahman, A. M., et al (2020), Grid integrated systems typically use a variable current scheme against a fixed voltage ac bus bar to inject electricity into the grid, the amount of which varies on the surrounding circumstances. Systems with one or three phases may integrate with the grid. To achieve the required voltage levels, transformers are installed between the produced ac voltage source and the integrating ac bus bar. Transformer less arrangements are also employed when the source side voltage level is sufficiently high relative to the integrating bus bar. Abdeslem Sahli and others (2019), The MPPT system, power conversion efficiency, and power quality are the key problems with solar power generating. Several research activities have been conducted with a focus on these three crucial factors, and numerous solution techniques have been proposed. Topological variants, various PWM techniques, and various control strategies are some of the many study areas. Abderezak Lahab and others (2020), The development of isolated DC sources derived from a single renewable energy source specifically for cascaded multi-level inverters, augmentable modular switching units, and similar issues for modular multi-level inverters are some of the aspects that are specifically addressed in research on topological variants. The numerous multicarrier sinusoidal PWM schemes, the space vector PWM schemes, and the step modulation schemes with selective harmonic elimination are some of the PWM systems that have undergone thorough investigation. The management of the whole operation, from the collection of renewable energy sources through the different stages of power conversion until the electricity is eventually integrated into the grid, is further governed by the control subsystems.

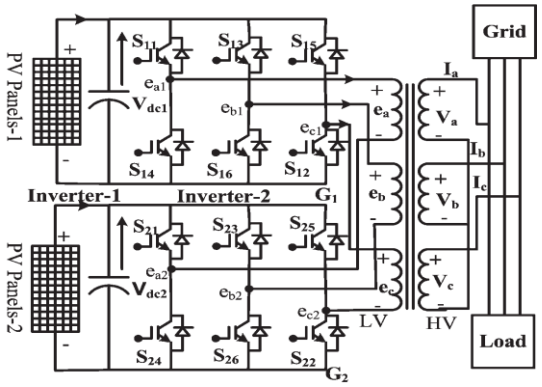

Fig:1.1 Power Circuit of the PV system with CTL1

2. SYSTEM CONFIGURATION

"MATHEMATICAL MODELING OF THE SYSTEM".

The characteristic equation of PV cells is given by

$$I = I_{ph} - I_s\left[\exp^{\frac{q(V+IR_s)}{nKT}} - 1\right] - \frac{V + R_s I}{R_{sh}}. \qquad (1)$$

The one from FIG. 2 is used in the simulation model in FIG (1). The parameters have values of 0.4 and 323, respectively. A PV array of (M N) PV modules can be constructed by connecting M single PV strings in parallel. The general equation of a multidimensional array model is given.

$$I = N_p\left[I_{ph} - I_s\left(\exp^{\frac{q\left[\left(\frac{V}{N_s}\right)+\left(\frac{I}{N_p}\right)R_s\right]}{KT}} - 1\right) - \frac{\left(\frac{V}{N_s}\right) + \left(\frac{I}{N_p}\right)R_s}{R_{sh}}\right]. \qquad (2)$$

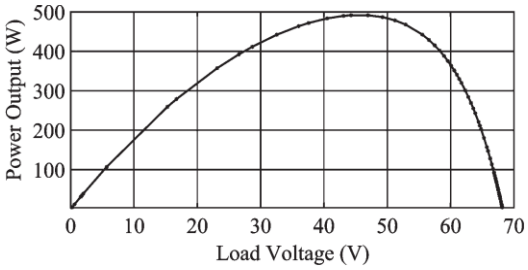

Fig: 2.1 Power –voltage characteristics for the PV cell

A. The maximum number of cells linked in series to produce a set and the maximum number of cells connected in parallel to form a series are both determined to be 48V under typical solar radiation conditions in India. The inverter's projected power rating is 2.5 kW. Fig. 3 displays the available output power at different output voltages. The constant maximum output power in this instance is 48V, which is maintained by continuous sun exposure. For the system to operate as effectively as possible,

the regulators are made to maintain the combined PV output voltage of the two inverters at 96V as illustrated in Fig. 1.

CTLI Model

The voltage across the a, b, and c windings for the power system under consideration is as follows:

$$e_a = \frac{2}{3}(e_{a1} - e_{a2}) - \frac{1}{3}(e_{b1} - e_{b2}) - \frac{1}{3}(e_{c1} - e_{c2}) \quad (3)$$

$$e_b = -\frac{1}{3}(e_{a1} - e_{a2}) + \frac{2}{3}(e_{b1} - e_{b2}) - \frac{1}{3}(e_{c1} - e_{c2}) \quad (4)$$

$$e_c = -\frac{1}{3}(e_{a1} - e_{a2}) - \frac{1}{3}(e_{b1} - e_{b2}) + \frac{2}{3}(e_{c1} - e_{c2}) \quad (5)$$

Here the first inverter pole voltages are ea1, eb1 and ec1 and the second inverter pole voltages are ea2, eb2 and ec2. For idealized power switches, the output voltage of CTLI can be expressed in matrix form as (3)-(5).

$$\begin{bmatrix} e_a \\ e_b \\ e_c \end{bmatrix} = \frac{1}{3}\begin{bmatrix} 2 & -1 & -1 \\ -1 & 2 & -1 \\ -1 & -1 & 2 \end{bmatrix}\begin{bmatrix} e_{a_1} \\ e_{b_1} \\ e_{c_1} \end{bmatrix} - \frac{1}{3}\begin{bmatrix} 2 & -1 & -1 \\ -1 & 2 & -1 \\ -1 & -1 & 2 \end{bmatrix}\begin{bmatrix} e_{a_2} \\ e_{b_2} \\ e_{c_2} \end{bmatrix}. \quad (6)$$

The SMC design should be effective in both gripping and gliding phases [15]–[20]. A button, also known as the switching function sij, is defined by the control rule given below: The six switching functions, ij, I 1, 2 and j 1, 2, 3, can be obtained as follows:

$$\gamma_{ij} = \begin{cases} 1, & \text{if } S_{ij} \text{ is ON } \overline{S_{ij}} \text{ OFF} \\ 0, & \text{if } S_{ij} \text{ is OFF } \overline{S_{ij}} \text{ ON.} \end{cases} \quad (7)$$

Consequently, the CTLI's three-phase output voltages were linked.

Control of vector The supply voltages' two-axis representation may be created as

$$\begin{bmatrix} V_\alpha \\ V_\beta \end{bmatrix} = \frac{2}{3}\begin{bmatrix} 1 & -1/2 & -1/2 \\ 0 & -\sqrt{3}/2 & \sqrt{3}/2 \end{bmatrix}\begin{bmatrix} V_a \\ V_b \\ V_c \end{bmatrix}. \quad (11)$$

Accordingly, (10) can be expressed as

$$\begin{bmatrix} V_\alpha \\ V_\beta \end{bmatrix} = \frac{2}{3}\begin{bmatrix} 1 & -1/2 & -1/2 \\ 0 & -\sqrt{3}/2 & \sqrt{3}/2 \end{bmatrix}\begin{bmatrix} \gamma_{1\alpha} \\ \gamma_{1\gamma} \end{bmatrix} V_{dc1} - \frac{2}{3}\begin{bmatrix} 1 & -1/2 & -1/2 \\ 0 & -\sqrt{3}/2 & \sqrt{3}/2 \end{bmatrix}\begin{bmatrix} \gamma_{2\alpha} \\ \gamma_{2\gamma} \end{bmatrix} V_{dc2}. \quad (12)$$

"Here, Vdc1 = Vdc2 = 48 V. The direct axis (d-axis) and the quadrature axis (q-axis) of the used vector control are derived following Fig. 4, and found as:".

$$\begin{bmatrix} V_d \\ V_q \end{bmatrix} = \begin{bmatrix} \sin\omega t & \cos\omega t \\ \cos\omega t & -\sin\omega t \end{bmatrix}\begin{bmatrix} V_m \sin\omega t \\ V_m \cos\omega t \end{bmatrix}. \quad (13)$$

A phase equivalent circuit is shown in FIG. The mains voltage is denoted by Va, the loss resistance by R, the leakage inductance of the transformer winding by L and the primary voltage of the transformer by n(ea1 ea2). A step-up transformer has a turns ratio of 1:1. Implementation of KVL in phases a, b and c.

$$n(e_{a1} - e_{a2}) = R_a i_a + L_a \frac{di_a}{dt} + V_a \quad (14)$$

$$n(e_{b1} - e_{b2}) = R_b i_b + L_b \frac{di_b}{dt} + V_b \quad (15)$$

$$n(e_{c1} - e_{c2}) = R_c i_c + L_c \frac{di_c}{dt} + V_c \quad (16)$$

The set point for the d-axis current is generated by the intermediate circuit voltage controller. In this study, the reference value of both DC voltages is kept constant at 96 V.

Sliding-Mode Control

Based on the current state of the state variables in the state space, the continuous state feedback control rule that makes up the SMC can quickly switch from one continuous structure to another. The dynamics of the system must be managed to execute the planned and directed [15]. SMC is particularly characterized by the following outstanding features:

Resilience, system order reduction [15–20], [28–30], and circuit breaker on/off behaviour adaptation are all important. The capacity to modify responses independently of system characteristics is one of the most significant aspects of the SM regime in VSS. Simple SM control using HB may be carried out without the need of extra computations or hardware. There are three fundamental techniques to maintain a consistent switching frequency for HM-based SM controllers [15]. 1) Properly developed constant ramp or timing controller functions. This control approach modifies the ramping/timing function to regulate a set switching frequency under all operational circumstances. 2) HM-based SM control with adaptive control to reduce switching frequency divergence 3) To offer SM controls with a consistent switching frequency, PWM may be utilised in addition to HM. In this paper, fundamental techniques for creating SMCs for CTLI are provided. The control problem may be resolved by using a cascade control structure composed of an inner current control loop and an outer voltage control loop. Utilizing the motion

separation characteristic of power converters via a cascade control technique simplifies control implementation even further. The dynamics of loop current and output voltage are used by power converters to govern rapid and slow motion, respectively. Power converters provide continuous regulation since they are by nature switching devices. Voltage controls are often designed using SM-PWM or hysteresis control, but current controls are frequently designed using conventional vector control methods. In this instance, the SM method is used to regulate the present mistake. The control goal is to keep the inverter capacitors' voltage control mechanism functioning. Control of the grid's active and reactive power generation is possible. This control approach was chosen because it fits the features of SM controllers like B. It is becoming a viable alternative to traditional ones because of its quick reaction time and strong resistance to outside disruptions. A control rule that informs the planning interface about the condition of the system prior to the chosen planning interface is taken into consideration while creating this SMC. Two switching methods are used to supply the gate signals for the first and second inverters, and they are each detailed below using HM approach.

I Two Level Circuit Scheme In this system, the bipolar modulation inverter has two output levels: 1 and 1. The switching logic is shown in Fig. 1 of FIG.

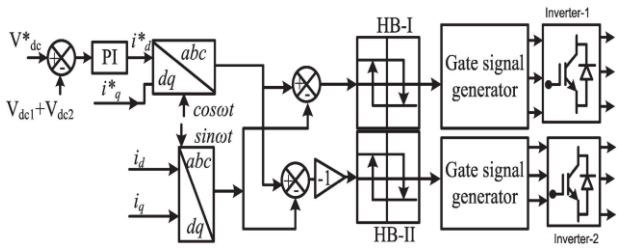

Fig:2.2 Control block diagram of scheme-1

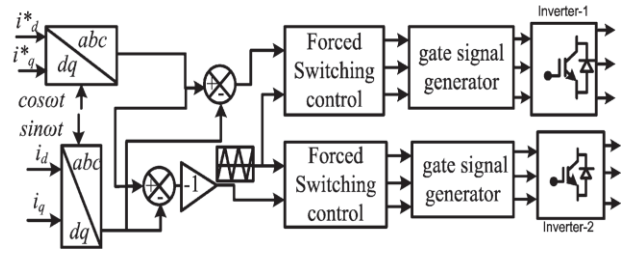

Fig:2.3 Control block diagram of scheme2

Two switches are activated throughout each cycle, while the other two are dormant, depending on the phase of the two inverters. PINv = k fsw, where fsw is the on-off switching loss whose frequency-dependent value is k. 2PInv is the total variable loss. Definition of variable structure control (u)

$$u = \begin{cases} +1, & \text{if } S_e > +\text{HB} \\ -1, & \text{if } S_e < -\text{HB} \end{cases} \qquad (20)$$

Se in this context refers to the difference between the state variable's actual value and the appropriate reference value. K is bigger than knob (Sk) in every shift and S meets the requirements of the SM theorem. Scheme I is shown in Figure 1 as previously mentioned. Schedule II FIG. 2 FORCING SWITCH Scheme II alludes to the plan. By contrasting the switching function with a fixed-frequency carrier signal, it is possible to calculate the switching frequency roughly. The carrier signal is shaped like a triangle. The triangular wave has an amplitude of HB. This method preserves the robust properties of the hysteresis controller while achieving steady switching frequency. At certain frequencies, the carrier signal is likewise constrained to a minimum amplitude. The inverter may reach complicated states if it is tiny. Tracking inaccuracy and settlement time both rise as container capacity grows. The suitable carrier size must thus be determined. The features of the SMC relating to reaction time and resilience to external shocks are taken into consideration while developing an SM controller (17). We explain the relative degrees of the controlled state variables id and iq using a canonical phase model (18). It is now feasible to create adequate slip surfaces to handle the id and iq variables since they are directly proportional to the feedback errors of the state variables. The discrepancy between the current references Ia, Ib, and Ic and the actual current is known as the feedback error.

3. RESULTS

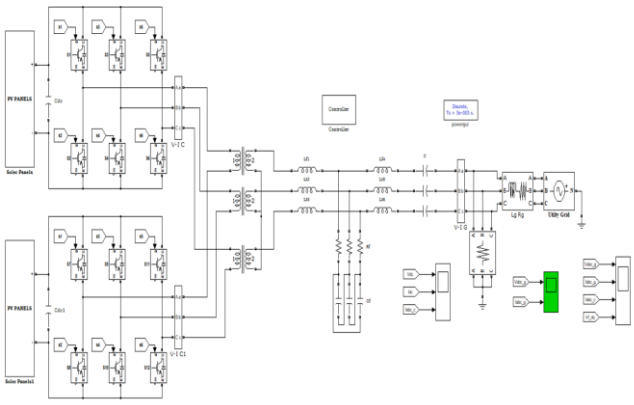

Fig 3.1 Simulation Block Diagram 1

A simulation circuit is used to demonstrate how the system is implemented. Bipolar modulation output levels for an inverter Two switches are used to turn a particular phase of the inverter on and off at different times during the cycle. If fsw is the switching frequency, the on-off switching loss is proportional to fsw.

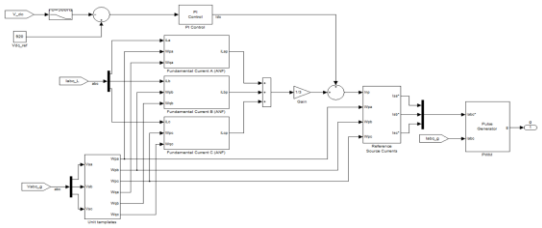

Fig 3.2 Simulation Block diagram 2

A simulation circuit illustrates the use of the control system. The switching frequency under consideration can be determined by comparing the switching function with a carrier signal at a fixed frequency. The carrier signal has a triangular shape. Amplitude of triangular signal at different frequencies

A smaller inverter leads to problematic switching states, and the larger the carrier size, the longer it takes to solve the tracking problem. The SM controller is constructed using a canonical model that accounts for the dynamics of the system and controls the state variables id and iq of relative degree 1 for response time and resilience to external shocks. Variable control is preferred over moving surfaces.

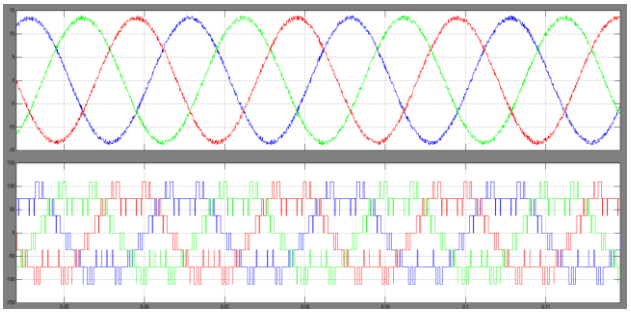

Fig 3.3 Voltage and current waveforms.

The simulation circuit displays the output voltage and current waveforms at the grid side as well as changes in solar radiation, converter voltage, and current.

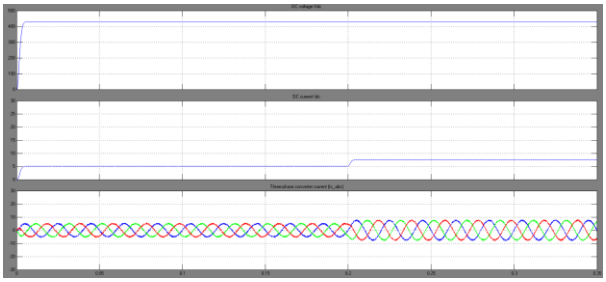

Fig 3.4 DC current and three phase current results

Simulated results for line to line voltage and line to line current are provided by line to line and line to current inverters.

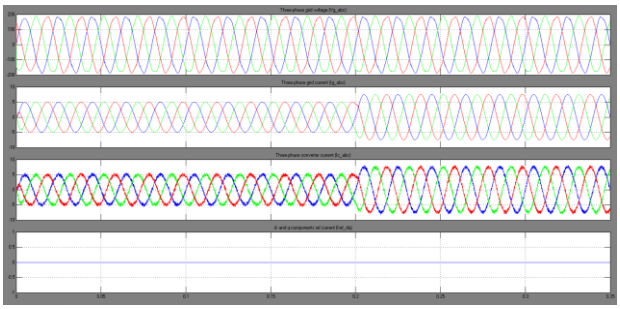

Fig:3.5 Three phase converted current and voltage

the two inverters' combined dc voltage during steady state operation and the two phase transformer output current.

4. CONCLUSION

In this study, grid-tied devices are controlled by a brand-new, dependable CTLI-based SM controller. In this circumstance, CTLI outperforms the other two SMC control strategies. The gate signals in Schemes I and II are produced using the HM and zero mean current error methods, respectively. Without or with solar radiation, it is certainly feasible to separate active and reactive power. By maintaining the DC link voltage at the optimal level for both schemes, a controller is shown that will increase the power produced by solar PV modules. Even with changing solar irradiance, variable inverter input power, and a 50% load increase, performance has been shown to remain dependable. The grid-connected PV system's THD is substantially lower than the switch-off limit, according the study. The DC connection voltage is maintained by both control systems while reactive power is sent to the grid in distributed STATCOM mode without solar radiation. The PV system generates active and reactive electricity because of the suggested SM controller. The dSPACE 1104 efficiently performs SMC in real time for a PV-based power system. The suggested controller's utility was shown by the high degree of agreement

between simulation and experiment results for the circumstances taken into account.

5. FUTURE SCOPE

Future applications for this approach could be adding battery and fuel cell power, or running them in both scenarios. To increase the switching efficiency and simplify the switching logic, the harmonic reduction can be further improved using artificial intelligence controls and the converter can be converted to a neutral-point-clamp NPC converter. In the long run, harmonic distortion is reduced.

6.REFERENECES

[1] J. M. Carrasco et al., "Power-electronic systems for the grid integration of renewable energy sources: A survey," IEEE Trans. Ind. Electron., vol. 53, no. 4, pp. 1002–1016, Jun. 2006.

[2] B. Sahan, S. V. Araújo, C. Nöding, and P. Zacharias, "Comparative evaluation of three-phase current source inverters for grid interfacing of distributed and renewable energy systems," IEEE Trans. Power Electron., vol. 26, no. 8, pp. 2304–2318, Aug. 2010.

[3] S. Kouro, J. I. Leon, D. Vinnikov, and L. G. Franquelo, "Grid-connected photovoltaic systems: An overview of recent research and emerging PV converter technology," IEEE Ind. Electron. Mag., vol. 9, no. 1, pp. 47–61, Mar. 2015.

[4] F. Blaabjerg, Z. Chen, and S. B. Kjaer, "Power electronics as efficient interface in dispersed power generation systems," IEEE Trans. Power Electron., vol. 19, no. 5, pp. 1184–1194, Sep. 2004.

[5] V. F. Pires, J. F. Martins, and C. Hao, "Dual-inverter for grid-connected photovoltaic system: Modeling and sliding mode control," Solar Energy, vol. 86, no. 7, pp. 2106–2115, Jul. 2012.

[6] A. Edpuganti and A. K. Rathore, "New optimal pulsewidth modulation for single DC-link dual-inverter fed open-end stator winding induction motor drive," IEEE Trans. Power Electron., vol. 30, no. 8, pp. 4386–4393, Aug. 2015.

[7] S. Kouro et al., "Recent advances and industrial applications of multilevel converters," IEEE Trans. Ind. Electron., vol. 57, no. 8, pp. 2553–2580, Aug. 2010.

[8] J. Rodríguez, J.-S. Lai, and F. Z. Peng, "Multilevel inverters: A survey of topologies, controls, and applications," IEEE Trans. Ind. Electron., vol. 49, no. 4, pp. 724–738, Aug. 2002.

[9] N. N. V. S. Babu, D. A. Rao, and B. G. Fernandes, "Asymmetrical dc link voltage balance of a cascaded two level inverter based STATCOM," in Proc. IEEE Region 10 Conf. (TENCON), Fukuoka, Japan, Nov. 2010, pp. 483–488.

[10] M. Malinowski, K. Gopakumar, J. Rodríguez, and M. A. Pérez, "A survey on cascaded multilevel inverters," IEEE Trans. Ind. Electron., vol. 57, no. 7, pp. 2197–2206, Jul. 2010.

AUTHOR'S PROFILE

Ms.Banapuram Anusha received her B.Tech from Institute of Electrical Engineering, Hyderabad in 2019. Presently she is pursuing M.Tech in Vidya Jyothi Institute of Technology, Hyderabad. Her areas of interest are Power System, Power Quality and Electrical Machines.

Email id: banapuram.anusha@gmail.com

Dr. C.N. Ravi completed his Bachelor of Engineering degree in Electrical and Electronics Engineering in the year 1999 from Crescent Engineering College, University of Madras, Chennai. Master of Engineering degree in Power System in the year 2006 from B.S.A.R Crescent Engineering College, Anna University, Chennai, and Ph.D in power system optimization techniques from Sathyabama University, Chennai, Tamilnadu,

India. At present he is working as professor in Vidya Jyothi Institute of Technology, Hyderabad, Telangana State, India. He has 16 years of teaching and 5 years of industrial experience. He received best teacher award in the year 2019, best researcher award in the year 2021 from ESN awards. One of his research scholar completed Ph.D. in Sathyabama University in January 2022. He has guided several UG and PG projects in the areas Power Electronics, Power systems and Electric Drives. His area of interest is power system optimization, FACTS, power electronics and renewable energy systems.

Email id: dr.ravicn@gmail.com